UNIVERSITY OF CALIFORNIA,

IRVINE

Enhancing Fluorescent Imaging Techniques: The Role of Silica Coating and Phasor Plot Analysis

THESIS

Submitted in partial satisfaction of the requirements

for the degree of

MASTER OF SCIENCE

In Biomedical Engineering

By

Alyssia Fossorier

Thesis Committee:

Professor Jered Haun, Chair

Professor Michelle Digman

Professor Abraham Lee

2024

TABLE OF CONTENTS

LIST OF FIGURES

LIST OF TABLES

ACKNOWLEDGEMENTS

I would like to thank my family and friends for their constant support and encouragement throughout my time at the University of California, Irvine (UCI). Their belief in me throughout this program has been the source of my motivation and strength to preserve through the rigorous curriculum.

I am also grateful to my Principal Investigator, Jered Haun, for allowing me to participate in his research, which has significantly expanded and strengthened my education. Under his guidance, I have gained valuable critical thinking skills that will enhance my candidacy for future career opportunities.

I had the privilege of being mentored by Hauna Lagouros and Tingwei Deng. Their mentorship has made me a stronger researcher and student. With these two PhD students as my guides, I have been able to seamlessly pursue my advanced education and strengthen my laboratory skills.

Overall, I am truly thankful for the invaluable experience I gained during my time at UCI. My education here has been a profoundly valuable journey.

ABSTRACT OF THE THESIS

Enhancing Fluorescent Imaging Techniques: The Role of Silica Coating and Phasor Plot Analysis

By

Alyssia Fossorier

Master of Science in Biomedical Engineering

University of California, Irvine, 2024

Professor Jered B. Haun, Chair

Cancer, particularly breast cancer, poses a significant global health challenge, affecting millions of women annually and remaining a leading cause of death. Early detection is crucial for improving outcomes, yet many cases go undiagnosed until advanced stages highlighting the need for accurate diagnostics. This thesis explores optical imaging and fluorescence lifetime imaging microscopy (FLIM) to enhance early detection in breast cancer.

Two key aspects of fluorescence imaging are focused on: enhancing the stability of fluorescent dyes, specifically quantum dots, through silica coating, and analyzing fluorescence lifetime using the phasor approach. Silica coating improves the stability and biocompatibility of quantum dots by acting as a protective barrier preserving their optical properties and preventing aggregation. The phasor approach in FLIM is used to analyze the behavior of fluorescent dyes, revealing distinct fluorophore positions on the phasor plot and providing insights into fluorescence decay and self-quenching.

Overall, the benefits of silica coating for dye stability and the insights gained through phasor plot analysis in FLIM can advance fluorescence imaging techniques. Future work should focus on applying these techniques to improve diagnostic accuracy in breast cancer analysis.

CHAPTER 1: INTRODUCTION

1.1 CANCER AND EARLY DETECTION

Cancer disrupts cell proliferation and apoptosis, leading to uncontrolled growth and tumor formation, particularly in breast cancer, a hormone induced heterogeneous disease influenced by factors like BRCA mutations, familial history, and lifestyle [1]. Breast cancer is the leading cause of death in women, with over 1.2 million new cases annually [2, 3]. Treatment typically involves surgery, chemotherapy, hormonal therapy, or radiotherapy [4, 5]. Early detection significantly improves survival rates, yet many cases remain undiagnosed until metastases occur, resulting in 90% of patient deaths [3]. Biomarkers, including nucleic acids and proteins, provide crucial insight into breast cancer risk, etiology, and prognosis[6]. While HER2, ER, and PR are common biomarkers, TNBC presents a challenge due to limited expression of these markers [7-8]. Accurate diagnostic techniques are essential for early detection and improving patient survival.

1.2 METHODS OF DIAGNOSTICS

Traditional anatomical imaging techniques including X-ray tomography (CT, positron emission tomography (PET), magnetic resonance imaging (MRI), and single photon emission computed tomography (SPECT) provide non-invasive screening, staging and tumor progression monitoring, offering critical insights into tumor physiology. However, these techniques vary in resolution, sensitivity, and cost-effectiveness, and involve potential risks of exposure to ionizing radiation [9].

Molecular imaging modalities (MI), including flow cytometry, fluorescence in situ hybridization (FISH), and immunohistochemistry (IHC), offer deeper insights into tumor

physiology at molecular and cellular levels. Flow cytometry analyzes cell surface markers, while FISH visualizes DNA or RNA sequences, and IHC detects specific proteins in tissue samples [10-12]. While MI provides improved diagnostic accuracy, these techniques cause sample destruction and lack the capacity for multiplexed data analysis. Optical imaging techniques can complement MI to enhance diagnostic capabilities further.

1.3 OPTICAL IMAGING AND IMMUNOFLUORESCENCE

Optical imaging is pivotal in advancing imaging techniques, utilizing light and photons to visualize cells within natural tissue without invasiveness. In breast cancer analysis, the technique measures metabolic changes indicating abnormal organ and tissue function early on [13,14]. Immunofluorescence employs fluorescent antibodies to explore cellular and molecular details, providing spatial information and insight into cellular signaling pathways. Multiplexing fluorescence imaging enhances this by detecting diverse cellular components simultaneously, yet faces challenges such as spectral overlap and tissue autofluorescence, necessitating improvements for streamlined analysis [15-17].

1.4 FLUORESCENCE LIFETIME IMAGING AND THE PHASOR APPROACH

Fluorescence lifetime imaging microscopy (FLIM) relies on the duration of fluorescent molecular emission after excitation, offering insight into molecular dynamics. When exposed to light, molecules absorb energy, exciting electrons to a temporarily higher energy level. As electrons are unstable at this higher energy level, they emit excess energy to return to the ground state. This emission duration defines the fluorescent lifetimes, which can be measured in either the time or frequency domain. The frequency domain, in particular, enables the detection of

multiple species through analysis in Fourier space. By using the frequency domain, overlapping fluorescence timelines in the time domain can be distinguished between different molecular species for a better understanding of molecular complexities and more accurate information [18,19].

The phasor approach, a powerful tool in FLIM analysis, transforms the fluorescence lifetime data into a frequency domain, allowing for the identification and characterization of multiple fluorescent species simultaneously. Overall, FLIM, in conjunction with the phasor approach, is an advantageous method of identifying biomarkers as the technique is a highly sensitive, simplistic, and non-invasive, multiplexing tool with the ability to study the diversity of protein location and morphology for accurate results for early detection of breast cancer.

To assist detection, fluorescence microscopy typically employs fluorescent probes to target specific structures or molecules within a sample, with nanomaterial probes such as quantum dots or fluorescent dyes offering distinct advantages over traditional molecular probes. These nanomaterials do not require amplification of the target protein, enabling rapid and direct analysis with high signal sensitivity, stability, multiplexing, and spatial mapping capabilities that hold great promise for a wide range of bio-imaging applications.

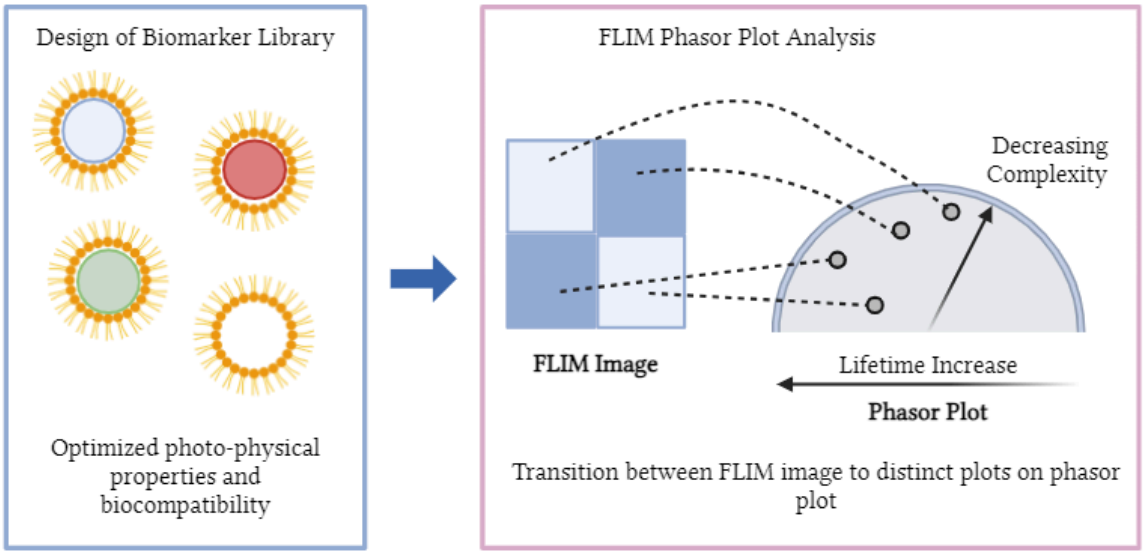

Figure 1**:** Creating nanoparticle probes for FLIM imaging for phasor plot analysis. Created in BioRender.com. Imaged based on Zrazhevskiy, P., Sena, M., & Gao, X. (2010). Designing multifunctional quantum dots for bioimaging, detection, and drug delivery. *Chemical Society reviews*

CHAPTER 2: STABILITY OF SILICA-COATED QUANTUM DOTS

2.1 BACKGROUND

Quantum dots (QDs) are semiconductor nanoparticles that have been extensively studied for their tunable and robust photoluminescent properties over the past three decades. In comparison to other nanoparticles, such as organic dyes, QDs are distinguished by their exceptional brightness, photostability, and high resistance to photobleaching, making them highly suitable for bio-imaging. Depending on their desired radius (1-5 nm), these particles can be engineered to emit specific fluorescence spectra ranging from ultraviolet (UV) to near-infrared (NIR) wavelengths. The brightness and photostability of QDs make them ideal for

long-term cellular imaging, offering high quantum yields and long fluorescent lifetimes. More importantly, their symmetric emission and broad absorption spectra enable multiplexed imaging by allowing simultaneous excitation and detection of multiple colors [20-23].

Although highly functional, the usage of QDs is limited by their potential cytotoxicity. QD toxicity can be caused by their physicochemical properties such as core-shell materials as the common elements used are cadmium (Cd), selenium (Se), and zinc (Zn) which are significantly damaging to cell culture and live animals. Additionally, the high-quality luminescence of QDs is stabilized using hydrophobic ligands which also create a cytotoxic effect [24, 25]. Thus a coating must be added to prevent these cytotoxic contaminations.

Silica (SiO_2) offers a robust solution to overcome challenges associated with quantum dots (QDs), providing stability, nontoxicity, and bioavailability. With low toxicity, strong chemical stability, and facile chemical modification, silica allows for tunable reactivity, optical transparency, and nonconductivity. Encapsulating QD cores with a silica shell mitigates issues related to photo and colloidal instabilities [24]. The reverse microemulsion method is commonly employed to effectively coat smaller molecules, such as QDs. In this process, water micelles dispersed in a continuous oil phase create an attraction between the polar head groups of the surfactant and aqueous phase droplets, while the hydrocarbon chains are attracted to the oil phase. Upon addition of silica, the precursor undergoes hydrolysis and condensation at the water-oil interface, promoting particle formation [24,26]. Evaluating the stability of silica-coated quantum dots under harsh environmental conditions aids in identifying limitations, thus enhancing their optimal utility.

As a therapeutic method of treating diseases, interest in chemical modification using polyethylene glycol (PEG) has significantly increased over the past 30 years. The process of

biochemically modifying bioactive molecules with PEG, known as PEGylation, reduces immunogenicity and enhances the nanoparticle's half-life, solubility, and stability. PEG consists of repeating units of ethylene glycol, and when conjugated to nanoparticles, each PEG molecule can interact with two or three water molecules, thereby increasing the hydrophilicity of nanoparticles and prolonging their retention time within the body without interfering with their function [27].

2.2 MATERIALS AND METHODS

i) Silica Coating of Quantum Dots

CdSe/ZnS Core-Shell Type Quantum Dots were purchased from NNCrystal US Corporation. Reagents used for silica coatings such as IGEPAL CO-520, ammonium hydroxide (NH_4OH), and Tetraethyl orthosilicate (TEOS) were also purchased from Sigma Aldrich while (2-diethylphosphatoethyl)triethoxysilane, tech (P-silane) and CarboxyethylSilanetriol, disodium salt, 25% in water (C-silane) were purchased from Gelst.

To coat quantum dots with silica, a reverse microemulsion method is employed. Individual vials are prepared, with each vial containing a mixture of cyclohexane (oil phase) and IGEPAL CO 520 (non-ionic surfactant), which is sonicated until clear. CdSe/ZnS are added to each vial at a volume of 200µL and sonicated for five minutes. Ammonium hydroxide is introduced as a catalyst, followed by the addition of tetraethyl orthosilicate (TEOS) to initiate the silica coating process. The reaction proceeds for 24 hours, after which carboxyethylSilanetriol (C-silane) and (2-diethylphosphatoethyl)triethoxysilane (P-silane) are added to each vial while stirring to reduce agglomeration and further functionalize the particles. Stirring continues for an additional 24 hours before proceeding to washing steps to finalize synthesis.

ii) Silica Nanoparticle Washing

In the washing process, the synthesized quantum dots are transferred to ten 1.5mL microcentrifuge tubes and mixed with methanol to dissolve impurities. The solutions are then centrifuged for 20 minutes, the supernatant is discarded, and 50% ethanol is added and sonicated until clear. The solutions are further filtered using Amicon Ultra-15 Centrifugal Filters -10K (from Sigma Aldrich) to remove aqueous impurities, repeating the process with 50% ethanol three times before finishing with a final wash using water. Throughout the washing steps, precise measurements of solvents, duration, and speed of centrifugation, and any specific temperature conditions are maintained to ensure thorough cleaning of quantum dots.

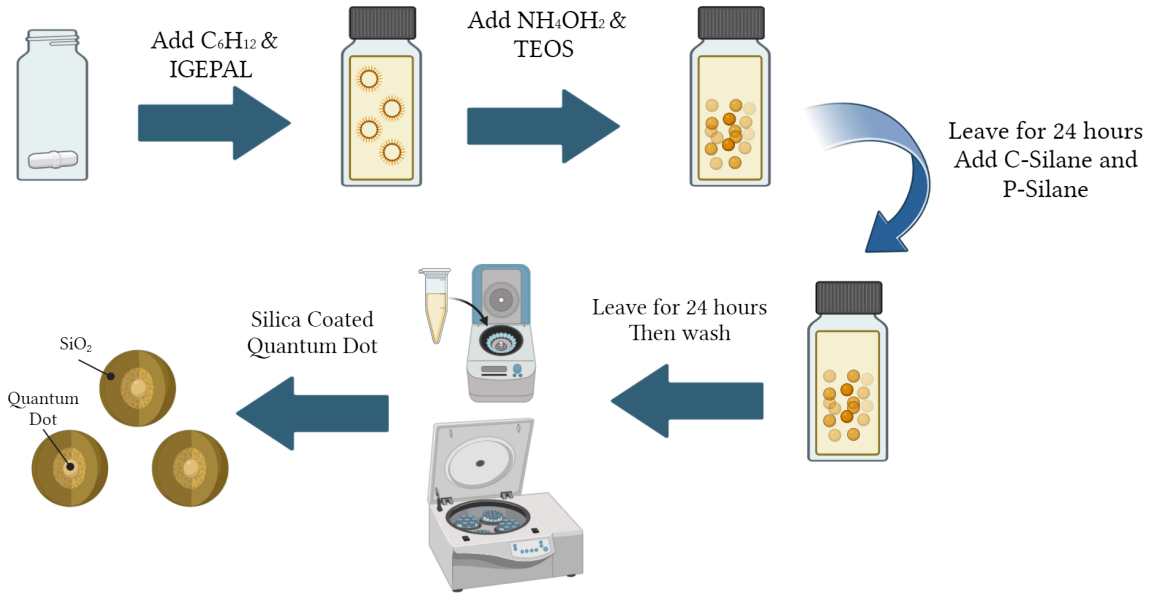

Figure 2: Schematic overview of the synthesis process of encapsulating quantum dots with silica using reverse microemulsion. Image created in BioRender.com

iii) Stability and Degradation Analysis

Bleach, known for its potent surface oxidation reactions due to its high sodium hypochlorite (NaClO) content, was used to investigate its effects on the silica coating of quantum dots. Various concentrations of bleach were mixed with water to create solutions for immersing the silica quantum dots. This immersion aimed to assess the stability and potential degradation of the silica coating over time.

The original uncoated quantum dots would be used as a control to compare the results of the silica coated quantum dots. The uncoated quantum dots were originally suspended with a solution containing toluene, which is a nonpolar solvent. To maintain the separation of the toluene coating and facilitate the degradation process of the quantum dots, a bleach solution with 50% ethanol was used. This ethanol content helps ensure that the bleach solution remains partially miscible with the toluene coating, allowing for the proper interaction with the quantum dots while preventing the complete mixing of the nonpolar toluene with the polar bleach solution.

The ISS Alba STED confocal lifetime imaging system with FLIM and Nikon Eclipse TE200-U microscope, located at the Laboratory for Fluorescence Dynamics (LFD) at the University of California, Irvine was used to calculate the photon count of the created quantum dot samples. To calibrate the imaging system, AlexaFluor555 was utilized as the reference dye.

iv) Size Analysis of Silica Quantum Dots

Dynamic Light Scattering (DLS) was used to measure the size distribution of silica quantum dots at the University of California, Irvine Laser Spectroscopy Lab. The technique

relies on the rate of Brownian motion, which is the random movement of particles due to collisions with surrounding solvent molecules. A laser beam is directed through the sample, and scattered light is collected at various angles by a detector, with backscatter detection set to an angle of 173 degrees to increase sensitivity for detecting nanoparticle size. By analyzing the fluctuations in scattered light intensity caused by Brownian motion, specifically using autocorrelation analysis, the size distribution of the suspended particles can be determined. For each sample, a disposable DLS cuvette was used during the analysis.

2.3 RESULTS AND DISCUSSION

2.3.1 SIZE ANALYSIS OF SILICA QUANTUM DOTS

Dynamic light scattering (DLS) was employed to assess the stability and size distribution of the synthesized particles. The results indicate a mono-disperse system, characterized by uniform size and minimal aggregation.

The data revealed that the synthesized silica particles had an average size of approximately 42.32 nm with a standard deviation of ± 2nm. Similarly, when suspended in phosphate-buffered saline (PBS), their average size was approximately 38.35 nm with a standard deviation of ± 2 nm.

The findings suggest that regardless of the medium (water or PBS), the size of the silica particles remained consistent and narrowly distributed. This indicates that the synthesis process yielded particles with uniform size characteristics, facilitating precise control over their size for various applications.

2.3.2 STABILITY AND DEGRADATION ANALYSIS OF SILICA QUANTUM DOTS

The results obtained from analyzing the photon count across varying concentrations of bleach decisively demonstrated that the silica coating effectively acted as a robust protective barrier for the quantum dots under harsh environmental conditions. Table 1 provides the collected values, indicating a decrease in fluorescence intensity for both coated and uncoated quantum dots with increasing bleach concentration, with the uncoated quantum dots exhibiting a more pronounced loss, suggesting their heightened susceptibility to damage. Figure 3 presents a comparative analysis of fluorescence intensity levels for both quantum dots at each bleach concentration, further supporting the protective benefits of the silica coating.

Bleach Concentration	Silica Coated (photon count)	Uncoated (photon count)
0.000%	700000	494000
0.00005%	343000	100000
0.00010%	339000	80000
0.00100%	322000	95000
0.03000%	320000	70000
0.12500%	47000	18000
0.50000%	8000	5000
1.00000%	200	1000

Table 1: The fluorescent intensity of the silica-coated quantum dots compared to the uncoated quantum dots in increasing concentrations of bleach

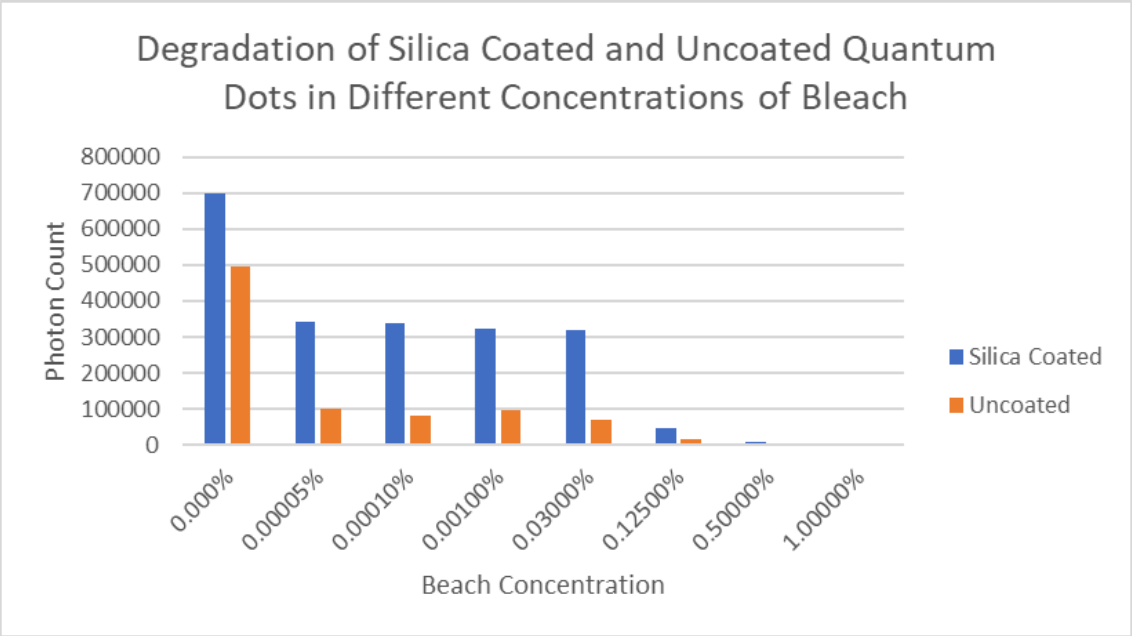

Figure 3: Bar chart representation of the silica-coated quantum dots compared to the uncoated quantum dots in increasing concentrations of bleach.

In line with these findings, at 1% bleach concentration, the uncoated quantum dots surprisingly exhibited a higher photon count. This unexpected anomaly is not attributable to the fluorescence of intact quantum dots, but likely arises from autofluorescence, an inherent property of damaged or degraded quantum dots. Autofluorescence occurs when quantum dots undergo structural damage or degradation, leading to the emission of fluorescence light without external excitation. The observed increase in photon count suggests extensive damage inflicted by the bleach on the majority of the uncoated quantum dots, highlighting the protective role of the silica coating in preserving the integrity of the particles under harsh conditions.

CHAPTER 3: CREATING A FLUORESCENT DYE LIBRARY

3.1 BACKGROUND

An obstacle when utilizing fluorescence imaging microscopy (FLIM) is the ability to analyze the complexity of multiple fluorescent species simultaneously. Normally, single fluorescent species can be characterized using a fitting curve. However, fluorescent mixtures contain different emission decays, varying in both function and magnitude, thus complicating and limiting multiplexing. The phasor approach provides a solution by transforming lifetime decay into the frequency space, thus eliminating the process of curve fitting of decay. By using each pixel in a FLIM image, different decay magnitudes appear at unique locations on a simple scatter plot. Pixels of single species appear on the curve of the phasor plot while mixtures are distributed within the plot based on the relative amounts of their components [28].

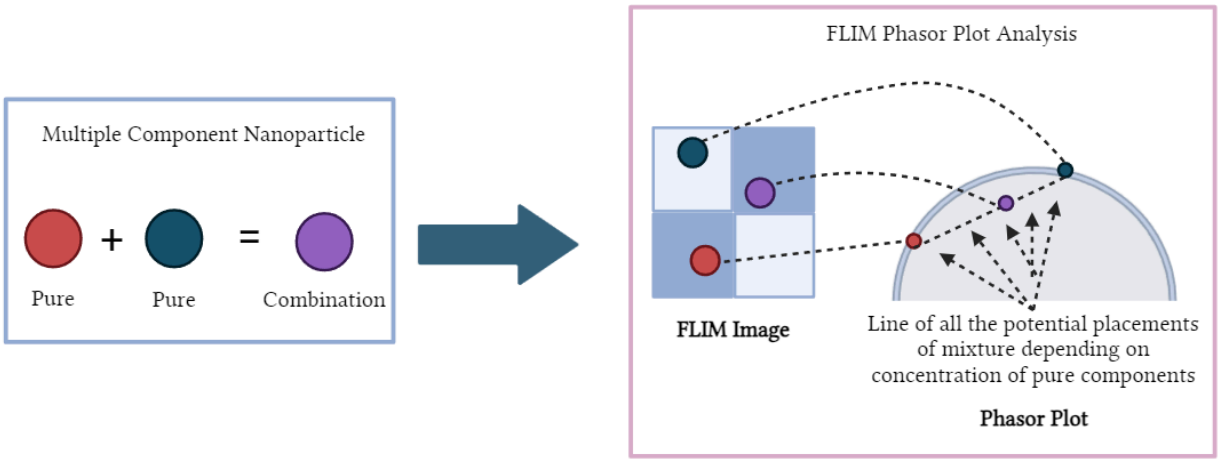

Figure 4**:** Visualization of differentiation of multiple components using phasor plot analysis. Created in BioRender.com.

3.2 MATERIALS AND METHODS

i) Silica Coating of Fluorescent Dyes

The methods for silica-coating fluorescent dyes follow the same process outlined in Chapter 2 but fluorophores are used instead of quantum dots. The fluorophores used are Bodipy, Rhodamine, Fsd, Atto, Ku530, and Dylight at concentrations of 120 µL, 60µL, 30µL, 10µL 3µL, and 1µL. Alexa Fluor 555 was used as a reference at the same concentrations.

ii) Silica Nanoparticle Washing

The materials and methods for washing the silica-coated fluorescent dyes follow the same procedures and materials used in Chapter 2.

iii) Emission of Fluorescent Dyes

The Cary Eclipse Fluorimeter and Cary-60 absorption spectrometer in the University of California, Irvine Spectroscopy Lab were used to measure the emission spectra of the synthesized silica quantum dots. For emission analysis, the detection range of the spectrometer was set to 550 nm to 650 nm, with an excitation wavelength of [actual] nm. The excitation wavelength was carefully chosen to prevent saturation of the detector by the emitted fluorescence, which could lead to inaccuracies in the measured fluorescence signal.

v) Fluorescence Lifetime Imaging (FLIM) Phasor Analysis

The fluorescence lifetime imaging of the synthesized fluorescence probes was examined using the phasor approach at the Laboratory for Fluorescence Dynamics (LFD) at the University of California, Irvine. The detection range for emission was fixed between 550 nm to 650 nm, with excitation spectra falling within the range of 510 nm to 550 nm. To calibrate the fluorescence probes, AlexaFluor555 was utilized as the reference dye.

3.3 RESULTS AND DISCUSSION

3.3.1 Emission of fluorescent dyes from self-quenching

Fluorescence analysis yielded consistent results across most fluorescent dyes, indicating a positive correlation between volume concentration and emission intensity, as illustrated in Figures 5-11. However, Bodipy dye (Figure 11) exhibited a different response. In contrast to the other dyes, Bodipy displayed a decrease in emission intensity at 120µL compared to 60µL, which contrasts the expected trend.

The deviation in Bodipy's emission behavior is likely attributed to self-quenching phenomena. Within the volume range of 60 to 120µL, the escalating concentration of fluorescent molecules surpassed a critical threshold, where self-quenching effects became significant. Consequently, the efficient emission of light was impeded, resulting in the observed decrease in emission intensity at higher concentrations.

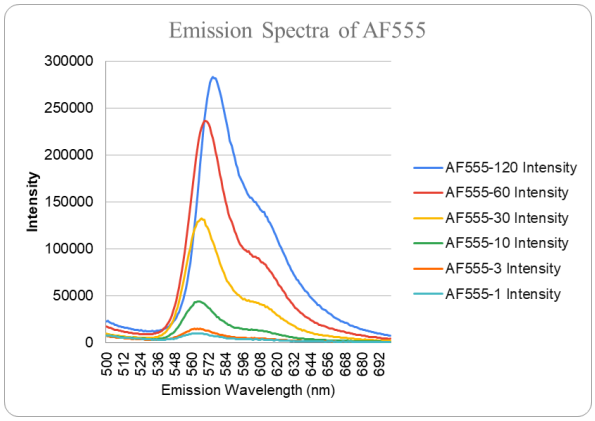

Figure 5: Emission of Af555

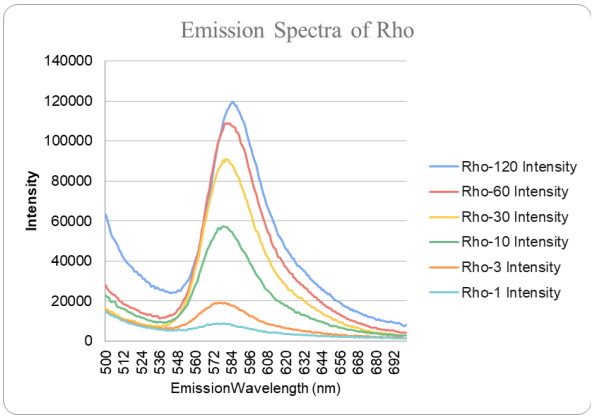

Figure 6: Emission of Rhodamine

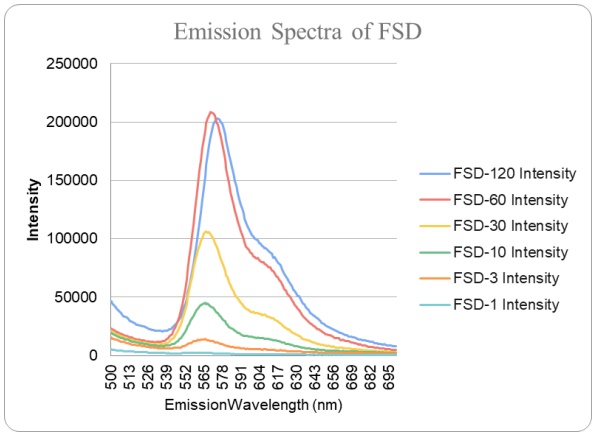

Figure 7: Emission of FSD

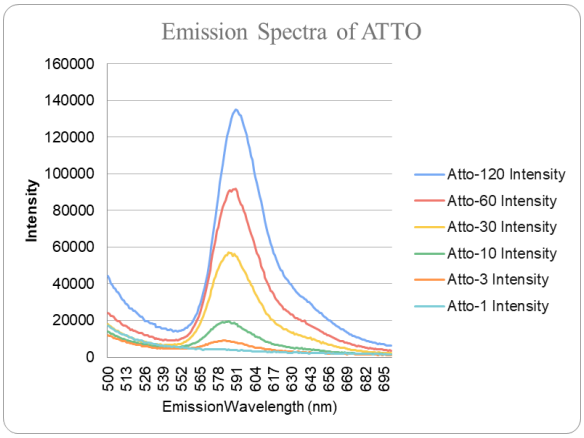

Figure 8: Emission of ATTO

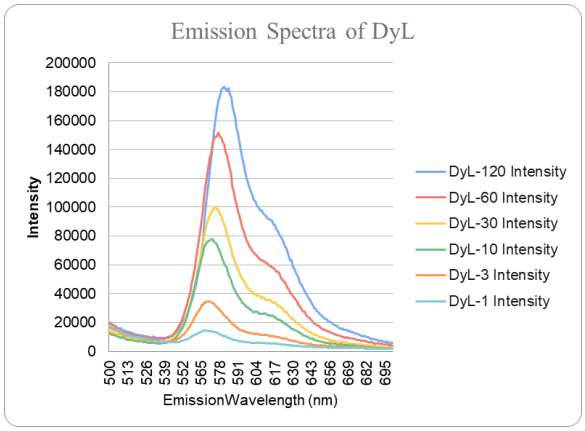

Figure 9: Emission of DyLite

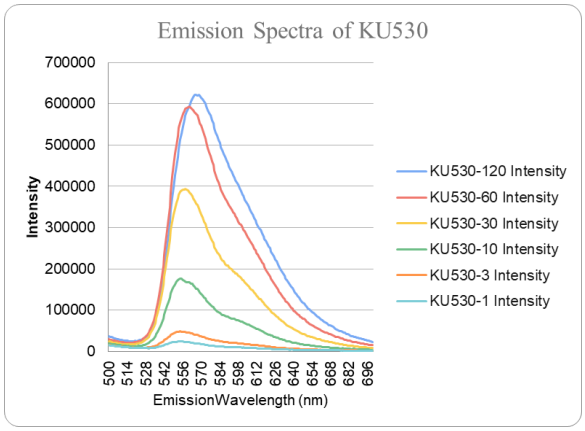

Figure 10: Emission of Ku530

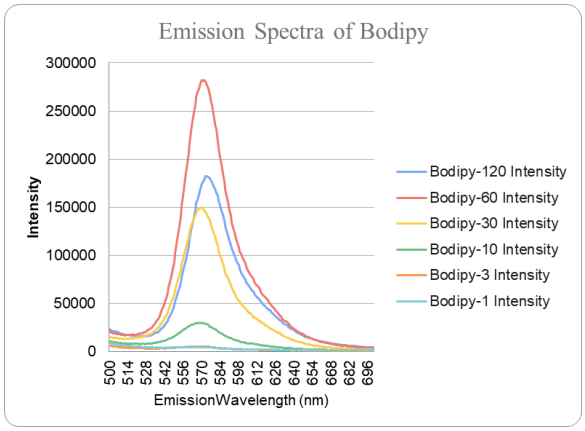

Figure 11: Emission Spectra of Bodipy with self-quenching occurring at 120uL

3.3.2 Phasor approach of fluorescent dyes from self-quenching

The phasor approach was employed to analyze the effects of fluorescent dyes at various concentration levels. Each dye used in the experiment was distinctly represented on the phasor plot, with positions determined by their respective fluorescence lifetimes. Notably, the right side of the semicircle corresponds to the shortest lifetimes. Self-quenching phenomena were observable on the phasor plot more distinctly through shifts in distribution caused by alterations in the fluorescence decay profile.

Ku530 displayed the lowest self-quenching efficiency, as evidenced by minimal shifts in its phasor position with increasing concentrations (Figure 12). The dye is positioned on the left side of the semi-circle indicating a high fluorescent lifetime. The positions of all volumes overlapping and remaining on the edge of the phasor plot suggest minimal deviation supporting the notion of low self-quenching efficiency for Ku530.

Bodipy, conversely, demonstrated higher self-quenching efficiency, as evident from the noticeable shifts in its phasor position with increasing concentration (Figure 12). Initially positioned on the edge of the phasor plot with a high fluorescent lifetime, the dye showed signs of self-quenching as 60μL was added, marked by a subtle but noticeable shift. This effect became more pronounced at 120μL, as depicted in Figure 11 (previous chapter), where significant self-quenching occurred. This is visually supported by the substantial shift in the dye's position towards the right, moving off the edge of the center. The movement of the dye at the volume of 120μL indicates self-quenching, which interferes with fluorophores, leading to decreased lifetime and increased complexity due to potential variations in emissions.

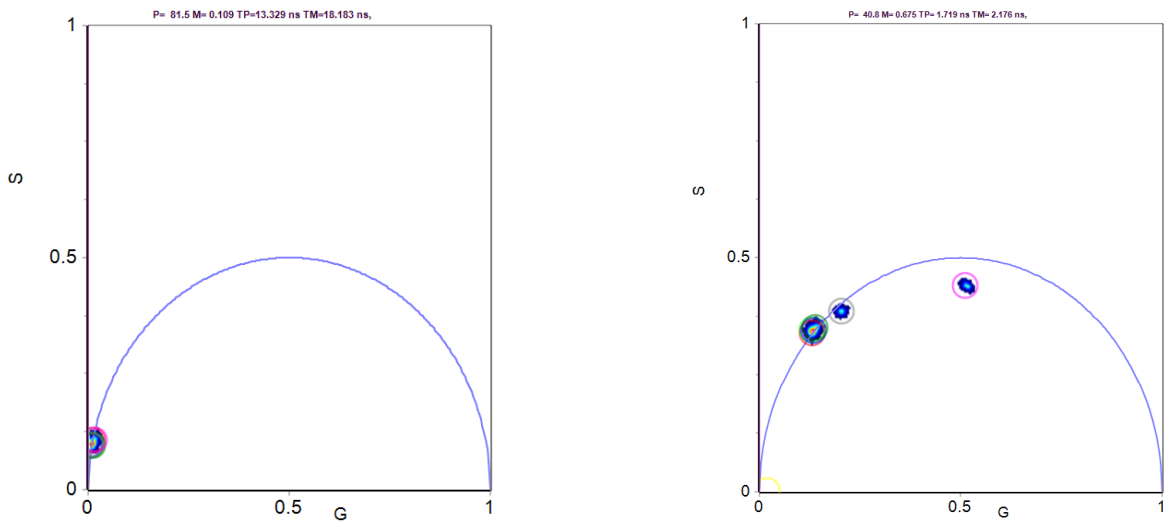

Figure 12: Fluorescence lifetime positions of Ku530 (left) and Bodipy (right) on phasor plot

1µL - Red, 3µL - Light Green, 10µL - Blue, 30µL - Dark Green, 60µL - Grey, 120µL - Pink

1µL - Red, 3µL - Light Green, 10µL - Blue, 30µL - Dark Green, 60µL - Grey, 120µL - Pink

The behavior of the remaining dyes (Atto, Rhodamine, Fsd, AF55, and Dylight) can be explained by self-quenching as their efficiency remains within the extremes of Ku530 and Bodipy. Atto overall has low self-quenching efficiency, but unlike Ku530 each increase in dye volume slightly shifts the position of the dye towards lower fluorescence lifetime with a more prominent shift at 120µL. Rhodamine, Fsd, AF555, and Dylight exhibit similar trends, showing a notable rise in self-quenching as the volume of dye increases. At each volume level, there is minimal overlap with others, causing a shift toward the right, indicating a lower fluorescent lifetime, and toward the center, suggesting increased complexity, with each incremental volume increase.

Overall, utilizing the phasor approach for fluorescence lifetime imaging offers a more robust analysis, as each probe occupies a distinct position on the graph. Minor alterations in fluorescence lifetime resulting from phenomena like self-quenching, aggregation, or impurities

are more accurately depicted on the phasor plot compared to an emission spectrum. The sensitivity of this method is evident in the analysis of not only significant results such as Ku530 or Bodipy, but in dyes such as Rhodamine, Fsd, Dylight, and AF555, where self-quenching is less prominent. Application of the phasor plot displays better trend indication of potential points of maximum self-quenching for these dyes.

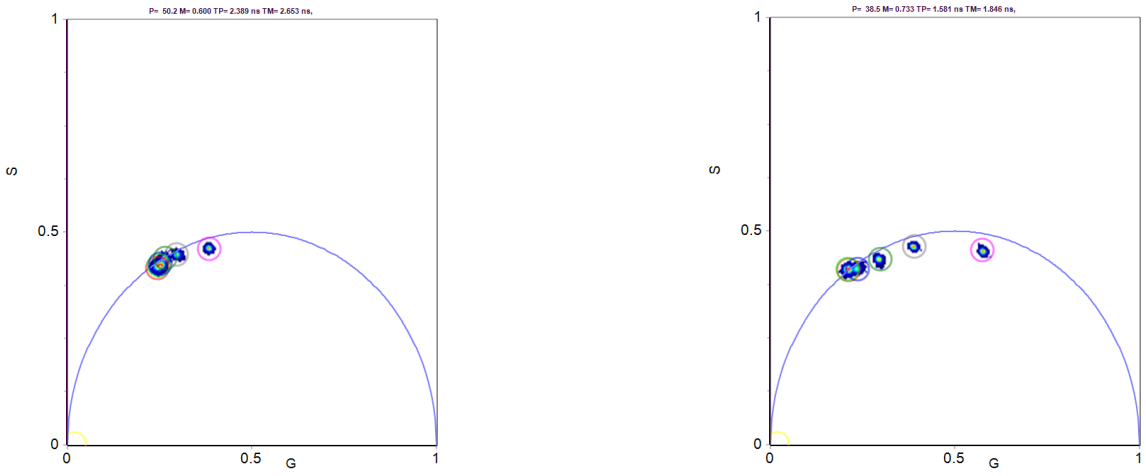

Figure 13: Fluorescence lifetime positions of Atto (left) and Rhodamine (right) on phasor plot

1µL - Red, 3µL - Light Green, 10µL - Blue, 30µL - Dark Green, 60µL - Grey, 120µL - Pink

1µL - Red, 3µL - Light Green, 10µL - Blue, 30µL - Dark Green, 60µL - Grey, 120µL - Pink

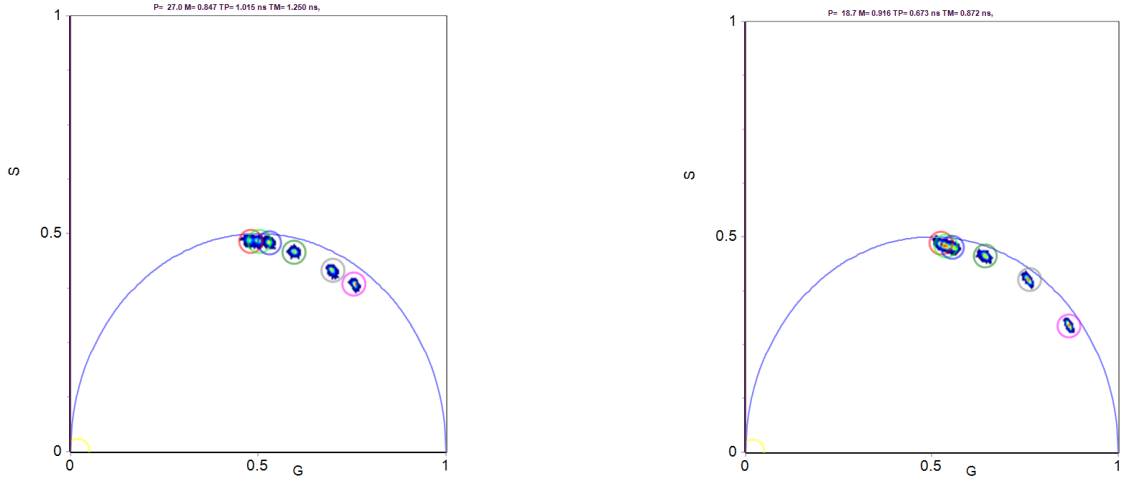

Figure 14: Fluorescence lifetime positions of Fsd (left) and AF555 (right) on phasor plot

1µL - Red, 3µL - Light Green, 10µL - Blue, 30µL - Dark Green, 60µL - Grey, 120µL - Pink

1µL - Red, 3µL - Light Green, 10µL - Blue, 30µL - Dark Green, 60µL - Grey, 120µL - Pink

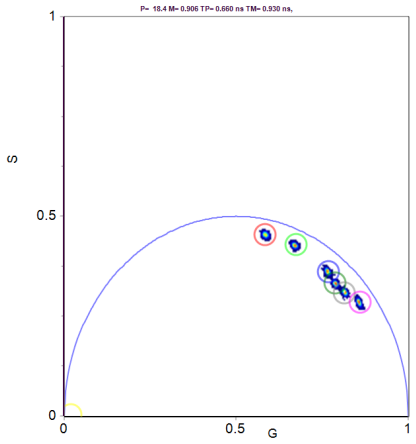

Figure 15: Fluorescence lifetime positions of Dylight on phasor plot

1µL - Red, 3µL - Light Green, 10µL - Blue, 30µL - Dark Green, 60µL - Grey, 120µL - Pink

CHAPTER 4: SUMMARY AND CONCLUSION

The first part of this thesis demonstrates the effectiveness of silica coating in enhancing the stability of fluorescent dyes, particularly quantum dots, even in harsh environmental conditions. When exposed to oxidative agents such as bleach, the silica coating serves as a protective barrier, shielding the surface of the particles from significant degradation. Notably, uncoated quantum dots exhibited a considerable decrease in fluorescence intensity at lower concentrations of bleach compared to their coated counterparts, providing clear evidence of the silica's role in preserving the optical properties of quantum dots. Furthermore, the silica coating

effectively prevented particle aggregation and improved biocompatibility, highlighting the coating's versatility in applications requiring robust and dependable fluorescent probes.

The second portion of the thesis illustrates how employing phasor plot analysis in fluorescent lifetime imaging (FLIM) reveals distinct positions of fluorophores, particularly regarding phenomena like self-quenching. As the total volume of dyes such as Ku530, Bodipy, Atto, Rhodamine, FSD, and Alexa Fluor 555 increased, the occurrence of self-quenching affected the trajectory of the dye positions. While the emission data hinted at the potential saturation of self-quenching, the phasor plot analysis provided a clearer indication of the trend toward maximum self-quenching. This analysis highlights the valuable insights gained through the phasor plot method in understanding the behavior of fluorophores under varying conditions.

Future work builds on these findings by developing an advanced diagnostic platform for high-content molecular analysis using color and lifetime data from fluorescent probes. This platform will implement a wide range of fluorescent probes with distinct spectral and lifetime characteristics, optimized to detect various breast cancer biomarkers with high specificity and sensitivity. An essential enhancement will be the implementation of silica coating, which will improve the probe's stability, biocompatibility, and functional versatility. Additionally, the incorporation of the phasor plot method will enhance data analysis, allowing for intuitive and precise interpretation of fluorescence lifetime imaging microscopy (FLIM) data. These advancements will ultimately provide more accurate characterization, improving patient outcomes through timely and precise intervention.

REFERENCES

[1] National Cancer Institute (2020). Cancer Statistics. *National Cancer Institute.* www.cancer.gov/about-cancer/understanding/statistics.

[2] Aznab, M., Izadi, B., Amirian, F., Khazaei, S., Madani, S. H., & Ramezani, M. (2022). Comparison of Immunohistochemical Methods (IHC) and Fluorescent in Situ Hybridization (FISH) in the Detection of HER 2 /Neu Gene in Kurdish Patients with Breast Cancer in Western Iran. *International journal of hematology-oncology and stem cell research*, *16*(4), 217–223. https://doi.org/10.18502/ijhoscr.v16i4.10879

[3] Li N., Jiang Y., Lv T., Li G., Yang F., (2022). Immunofluorescence analysis of breast cancer biomarkers using antibody-conjugated microbeads embedded in a microfluidic-based liquid biopsy chip. *Biosensors and Bioelectronics, 216*. https://doi.org/10.1016/j.bios.2022.114598

[4] Shahbazi, N., Zare-Dorabei, R., Morteza Naghib, S. (2021). Multifunctional nanoparticles as optical biosensing probe for breast cancer detection: A review, *Materials Science and Engineering: C Volume 127* https://doi.org/10.1016/j.msec.2021.112249.

[5] Chinen, A. B., Guan, C. M., Ferrer, J. R., Barnaby, S. N., Merkel, T. J., & Mirkin, C. A. (2015). Nanoparticle Probes for the Detection of Cancer Biomarkers, Cells, and Tissues by Fluorescence. Chemical reviews, 115(19), 10530–10574. https://doi.org/10.1021/acs.chemrev.5b00321

[6] Sarhadi, V. K., & Armengol, G. (2022). Molecular Biomarkers in Cancer. *Biomolecules*, *12*(8), 1021. https://doi.org/10.3390/biom12081021

[7] Ahn, S., Woo, J. W., Lee, K., & Park, S. Y. (2020). HER2 status in breast cancer: changes in guidelines and complicating factors for interpretation. *Journal of pathology and translational medicine*, *54*(1), 34–44. https://doi.org/10.4132/jptm.2019.11.03

[8] Dou W., Liu L., Gao J., Cheng G., Field R., James T., Li J., He X. (2018). Fluorescence imaging of a potential diagnostic biomarker for breast cancer cells using a peptide-functionalized fluorogenic 2D material. Chemical Communications 88. https://doi.org/10.1039/C9CC06399D

[9] Drescher, H., Weiskirchen, S., & Weiskirchen, R. (2021). Flow Cytometry: A Blessing and a Curse. Biomedicines, 9(11), 1613. https://doi.org/10.3390/biomedicines9111613

[10] Shakoori A. R. (2017). Fluorescence In Situ Hybridization (FISH) and Its Applications. Chromosome Structure and Aberrations, 343–367. https://doi.org/10.1007/978-81-322-3673-3_16

[11] Gozzetti, A., & Le Beau, M. M. (2000). Fluorescence in situ hybridization: uses and limitations. Seminars in hematology, 37(4), 320–333. https://doi.org/10.1016/s0037-1963(00)90013-1

[12] Zaha D. C. (2014). Significance of immunohistochemistry in breast cancer. World journal of clinical oncology, 5(3), 382–392. https://doi.org/10.5306/wjco.v5.i3.382

[13] Priovano, G., Roberts S., Kossatz S., Reiner T., (2020). Optical Imaging Modalities: Principles and Applications in Preclinical Research and Clinical Settings. Journal of Nuclear Medicine, 1419-1427; DOI: 10.2967/jnumed.119.238279

[14] National Institute of Biomedical Imaging and Bioengineering (NIBIB). “Optical Imaging.” National Institute of Biomedical Imaging and Bioengineering, U.S.

Department of Health and Human Services, Dec. 2020, www.nibib.nih.gov/science-education/science-topics/optical-imaging.

[15] Stadler, C., Rexhepaj, E., Singan, V. *et al.* Immunofluorescence and fluorescent-protein tagging show high correlation for protein localization in mammalian cells. *Nat Methods* 10, 315–323 (2013). https://doi.org/10.1038/nmeth.2

[16] Im K, Mareninov S, Diaz MFP, Yong WH. An Introduction to Performing Immunofluorescence Staining. Methods Mol Biol. 2019;1897:299-311. doi: 10.1007/978-1-4939-8935-5_26. PMID: 30539454; PMCID: PMC6918834.

[17] Bodenmiller B. (2016). Multiplexed Epitope-Based Tissue Imaging for Discovery and Healthcare Applications. Cell systems, 2(4), 225–238. https://doi.org/10.1016/j.cels.2016.03.008

[18] Datta, R., Heaster, T. M., Sharick, J. T., Gillette, A. A., & Skala, M. C. (2020). Fluorescence lifetime imaging microscopy: fundamentals and advances in instrumentation, analysis, and applications. *Journal of biomedical optics*, *25*(7), 1–43. https://doi.org/10.1117/1.JBO.25.7.071203

[19] Combs C. A. (2010). Fluorescence microscopy: a concise guide to current imaging methods. *Current protocols in neuroscience*, *Chapter 2*, Unit2.1. https://doi.org/10.1002/0471142301.ns0201s50

[20] Shishodia, S., Chouchene, B., Gries, T., & Schneider, R. (2023). Selected I-III-VI2 Semiconductors: Synthesis, Properties and Applications in Photovoltaic Cells. *Nanomaterials (Basel, Switzerland)*, *13*(21), 2889. https://doi.org/10.3390/nano13212889

[21] Zrazhevskiy, P., Sena, M., & Gao, X. (2010). Designing multifunctional quantum dots for bioimaging, detection, and drug delivery. *Chemical Society reviews*, *39*(11), 4326–4354. https://doi.org/10.1039/b915139g

[22] Herrera, V., , Hsu, S. J., , Rahim, M. K., , Chen, C., , Nguyen, L., , Liu, W. F., , & Haun, J. B., (2019). Pushing the limits of detection for proteins secreted from single cells using quantum dots. The Analyst, 144(3), 980–989. https://doi.org/10.1039/c8an01083h

[23] Resch-Genger, U., Grabolle, M., Cavaliere-Jaricot, S. *et al.* Quantum dots versus organic dyes as fluorescent labels. *Nat Methods* 5, 763–775 (2008). https://doi.org/10.1038/nmeth.1248

[24] Pham, X. H., Park, S. M., Ham, K. M., Kyeong, S., Son, B. S., Kim, J., Hahm, E., Kim, Y. H., Bock, S., Kim, W., Jung, S., Oh, S., Lee, S. H., Hwang, D. W., & Jun, B. H. (2021). Synthesis and Application of Silica-Coated Quantum Dots in Biomedicine. *International journal of molecular sciences*, *22*(18), 10116. https://doi.org/10.3390/ijms221810116

[25] Nikazar, S., Sivasankarapillai, V. S., Rahdar, A., Gasmi, S., Anumol, P. S., & Shanavas, M. S. (2020). Revisiting the cytotoxicity of quantum dots: an in-depth overview. *Biophysical reviews*, *12*(3), 703–718. https://doi.org/10.1007/s12551-020-00653-0

[26] Naurafkan, E., Gao H., Hu, Z., Wen, D., (2017). Formulation optimization of Reverse microemulsions using design of experiments for nanoparticle synthesis. *Chemical Engineering Research and Design,125*, 367-384.

[27] Gupta, V., Bhavanasi, S., Quadir, M., Singh, K., Ghosh, G., Vasamreddy, K., Ghosh, A., Siahaan, T. J., Banerjee, S., & Banerjee, S. K. (2019). Protein PEGylation for cancer

therapy: bench to bedside. *Journal of cell communication and signaling*, 13(3), 319–330. https://doi.org/10.1007/s12079-018-0492-0

[28] Rahim M., Zhao J., Patel H., Lagouros H., Kota R., Fernandez I., Gratton E., and Haun J., (2022), Phasor Analysis of Fluorescence Lifetime Enables Quantitative Multiplexed Molecular Imaging of Three Probes, *Analytical Chemistry* 94 (41), 14185-14194 DOI: 10.1021/acs.analchem.2c02149